

Surface Properties and Biocompatibility of Cellulose Acetates

Adina Maria Dobos, Iuliana Stoica, Nicolae Olaru, Liliana Olaru, Emil Ghiocel Ioanid, Silvia Ioan

"Petru Poni" Institute of Macromolecular Chemistry, Iasi 700487, Romania

Received 2 August 2011; accepted 14 October 2011

DOI 10.1002/app.36361

Published online 28 January 2012 in Wiley Online Library (wileyonlinelibrary.com).

ABSTRACT: The article describes some properties of cellulose acetates (CAs) with different substitution degrees. The hydrophilic/hydrophobic properties, morphological aspects, and interface properties with red blood cells and platelets are affected by the substitution degree, synthesis conditions, history of the formed films from solutions in acetone/water nonsolvent/nonsolvent mixtures, and low pressure plasma

treatment. The results obtained are useful in biomedical applications, including evaluation of bacterial adhesion onto surfaces, or utilization of CA for semipermeable membranes. © 2012 Wiley Periodicals, Inc. *J Appl Polym Sci* 125: 2521–2528, 2012

Key words: polysaccharides; hydrophilic polymers; biocompatibility; biological applications of polymers

INTRODUCTION

Typical research and application areas of polymeric biomaterials include tissue replacement, tissue augmentation, tissue support, and drug delivery. In many cases, the body needs only the temporary presence of a device/biomaterial, in which instantly-biodegradable and certain partially biodegradable polymeric materials are better alternatives than the biostable ones. Recent treatment concepts of scaffold based on tissue engineering principles differ from standard tissue replacement and drug therapies, as the engineered tissue aims not only to repair but also to regenerate the target tissue. Cells have been cultured outside the body for many years; however, it has only recently become possible for scientists and engineers to grow complex three-dimensional tissue grafts to meet clinical needs. New generations of scaffolds based on synthetic and natural polymers are being developed and evaluated at rapid pace, aimed at mimicking the structural characteristics of the natural extracellular matrix.¹

The natural abundance and biodegradability of cellulose, together with its ability to provide unique properties through diversification of cellulosic structures determine a wide range of applications. In their native form, cellulosic materials have been widely used in the manufacture of optical products, such as hard contact lenses, due to their excellent clarity, good wettability and high gas permeability,

textile fibers, molding powder sheets, optical membranes, etc. In addition, cellulose derivatives evidence excellent properties. Usually, this material is molded and extruded into various consumer products, such as brush handles, tool handles, toys, steering wheels, or other items. Cellulose acetates (CAs) are used in lacquers and protective coatings for various substrates including paper, glass, metal, leather, and wood. Furthermore, photographic and cinematographic films, as well as X-ray films, microfilms, and graphic films, are made from CA. Special castings of CA films are also used for water purification, blood purification dialysis, air separation, and for a large range of biotechnological applications.

On the other hand, adhesion of red blood cells, platelets or water to the CA substrate plays a crucial role in biomedicine. For analyzing the biocompatibility of CA with different substitution degrees, the relations between the physico-chemical properties of material surface and the adhesion of blood components should be known. Surface wettability, which is associated with surface free energy, has often been related to cell adhesion phenomena.^{2,3} In order to study the red blood cells, platelets, or water adhesion as a function of the substitution degree, it is preferable to compare a chemically homologous series of polymers for minimizing the contribution of specific interactions between adherent cells and chemical groups at the solid surface.

Gas plasma or glow discharge treatment is currently used for surface modification of materials, particularly to improve either the hydrophobicity or hydrophilicity of substrates.^{4,5} Low-pressure plasma treatment causes significant changes in the surface tension of a polymer. However, the three main

Correspondence to: S. Ioan (ioan_silvia@yahoo.com).

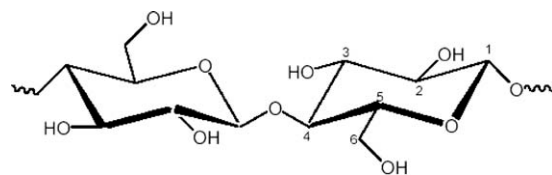
TABLE I
Hydrolysis Conditions of Cellulose Acetates in Homogeneous Systems⁸

Conditions/code ^a	CA _{1.73}	CA _{1.88}	CA _{1.90}	CA _{2.21}
T (°C)	60	40	40	40
Time (h)	24	19 (phase 1) 20 (phase 2)	35	63
Composition (wt %)				
Acetic acid	57	90	90	98
Water	8	10 (phase 1) 10 (phase 2)	10	2
Benzene	35	–	–	–
H ₂ SO ₄ (wt %)	10	10	10	10

^a Subscripts denote the substitution degrees.

groups of processes that should be considered for analysis are: polymer etching (involving a large set of destructive reactions which remove the surface material and can enlarge pore diameter), modification of surface chemistry (i.e., alteration of surface chemistry through changes in functionalities), and plasma polymer deposition (including processes allowing deposition of materials on the surface as a thin layer).⁶ It is also known that gas plasma modification of polymer surfaces has been used to gradually increase wettability on the adhesion of endothelial cells.⁷

In a previous article,⁸ the homogeneous hydrolysis of highly acetylated cellulose was studied in the presence or absence of a hydrocarbon (toluene, benzene), besides acetic acid and water, with sulfuric acid as a catalyst. The conformational behavior and the unperturbed dimensions of CA with different substitution degrees were investigated by viscometry and interferometry in 2-methoxyethanol and acetone/water solvent mixtures. The influence of concentration and temperature on coil densities and dimensions, as well as that of solvent mixtures composition on the solution properties were discussed.⁹ Also, rheology results showed a sol–gel behavior, a case in which the specific properties are modified as a function of solvent mixture composition. Gelation occurs as a result of nonsolvents-induced polymer aggregation and macromolecular association formation.¹⁰ Also, the structural characteristics of CA



Scheme 1 Chemical structure of cellulose.

membranes were discussed in correlation with different properties,¹¹ for obtaining materials with potential applications.

The objective of the present study was to provide information concerning the influence of the substitution degrees, history of membrane preparation from the casting solutions, and low-pressure plasma treatment on the surface properties of CA. The results were correlated with the hydrophilic/hydrophobic properties and compatibility of red blood cells and platelets, for extending the possible CA biomedical applications.

EXPERIMENTAL

Materials

CA with different substitution degrees, and number average molecular weight of 40,000 was synthesized from cellulose (Buckeye Cellulose Corporation, Memphis, TN), in both conventional media (acetic acid/water) (CA_{1.88} and CA_{1.90} samples) and an acetic acid/water/benzene system (CA_{1.73} sample), using the compositions presented in Table I, as described in detail elsewhere.⁸ Modification of the hydrolysis bath composition gave CA with different substitution degrees and different substitutions of the hydroxyl groups on both the primary (C₆) and secondary (C₂ and C₃) carbon atoms positions (Scheme 1). Localizations of the acetyl groups cause differences in the supramolecular structures of the samples.¹²

The membranes used for surface tension and atomic force microscopy (AFM) investigations were prepared from CA solutions of 10 g/dL concentration, in acetone/water nonsolvent/nonsolvent mixtures. According to Table II, CA possess different

TABLE II
Huggins Constants and Plot Regressions, r^2 , for Cellulose Acetates with Different Substitution Degrees, as a Function of the Volume Fraction of Acetone, ϕ_1 , at 25°C⁹

DS	ϕ_1									
	0.75		0.80		0.85		0.90		0.95	
	k_H	r^2	k_H	r^2	k_H	r^2	k_H	r^2	k_H	r^2
1.73	–	Small	–	Small	0.656	0.998	Insoluble		Insoluble	
1.88	–	Small	–	Small	0.548	0.891	Insoluble		Insoluble	
1.90	0.940	0.940	0.628	0.750	1.138	0.986	Insoluble		Insoluble	
2.21	Insoluble		Insoluble		0.848	0.940	0.829	0.970	0.893	0.999

TABLE III
Contact Angle of Different Test Liquids, θ , in ($^\circ$),
for Untreated and Treated Samples

Sample	Untreated samples				Treated sample		
	W	F	CH ₂ I ₂	1-Bn	F	CH ₂ I ₂	1-Bn
CA _{1.73}	64.0	42.0	36.0	16.5	7.3	16.0	6.0
CA _{1.88}	56.0	52.5	35.0	25.0	6.0	16.5	9.0
CA _{1.90}	47.5	32.5	34.5	21.5	9.0	17.0	11.0
CA _{2.21}	52.5	50.0	31.0	16.5	9.0	19.0	10.5

domain of solubility, depending on the substitution degrees. For this reason, the compositions of nonsolvent mixtures used in the paper are 0.15, 0.25, 0.25, and 0.10% vol, for CA_{1.73}, CA_{1.88}, CA_{1.90}, and CA_{2.21}, respectively (see previous studies).^{9,10}

The polymer solutions were cast on a glass plate and initially solidified by slow drying in saturated atmosphere of the used solvent, and finally in vacuum, at 30°C. Thus prepared, the CAs membranes were subjected to surface analysis, before and after plasma treatment.

Measurements

Contact angle

For contact angle measurements, a 2 μ L uniform drop of the test liquid was deposited on the film surface and the contact angles were measured after 30 s, using a video-based optical contact angle measuring device equipped with a Hamilton syringe, in a temperature-controlled environmental chamber. All measurements were performed in the atmosphere, at a temperature of 25°C.

AFM images were obtained on a SPM SOLVER Pro-M instrument. A NSG10/Au Silicon tip with a 35 nm curvature radius and 255 kHz oscillation mean frequency was used to investigate membrane surface morphology. The device was operated in semi-contact mode, over 10 \times 10 μ m scan areas, 256 \times 256 scan point size images being thus obtained. The differences in membrane surface morphology were expressed in terms of various roughness parameters, such as root-mean-square roughness (rms)—which represents the mean value of the surface relative to the center plane, nodule height from the height profile (nhp), nodules average weight from the histogram (nhh), and number of pores (*N*) with their characteristics: area, volume, depth, and diameter.

RESULTS AND DISCUSSION

Surface tension properties

The methods used for the determination of surface tensions are based on contact angle measurements

between the liquid (water) meniscus and the CA surface membranes treated or untreated in low-pressure cold plasma. A contact angle below 90° indicates that the substrate is readily wetted by the test liquid, while an angle over 90° shows that the substrate will resist wetting. Table III lists the contact angles between double-distilled water, formamide, methylene iodide, and 1-brom-naphthalene, and the CA samples.

The experimental data for surface tension components were obtained by the acid/base method (LW/AB), [eqs. (1)–(4)],¹³ using the known surface tension components of different liquids listed in Table IV,^{14–18} and the contact angles from Table III:

$$1 + \cos \theta = \frac{2}{\gamma_{lv}} \cdot \left(\sqrt{\gamma_{sv}^d \cdot \gamma_{lv}^d} + \sqrt{\gamma_{sv}^+ \cdot \gamma_{lv}^-} + \sqrt{\gamma_{sv}^- \cdot \gamma_{lv}^+} \right) \quad (1)$$

$$\gamma_{sv}^p = 2 \cdot \sqrt{\gamma_{sv}^+ \cdot \gamma_{sv}^-} \quad (2)$$

$$\gamma_{sv} = \gamma_{sv}^d + \gamma_{sv}^p \quad (3)$$

$$\gamma_{sl} = \left(\sqrt{\gamma_{sv}^d} - \sqrt{\gamma_{lv}^d} \right)^2 + 2 \left(\sqrt{\gamma_{sv}^+ \gamma_{sv}^-} + \sqrt{\gamma_{lv}^+ \gamma_{lv}^-} - \sqrt{\gamma_{sv}^+ \gamma_{lv}^-} - \sqrt{\gamma_{sv}^- \gamma_{lv}^+} \right) \quad (4)$$

where superscripts “*d*” and “*p*” indicate the disperse and the polar component obtained from the γ_{sv}^- electron-donor and the γ_{sv}^+ electron-acceptor interactions, while γ_{sl} indicates the solid–liquid interfacial tension.

As to eq. (1) (the acid/base method), literature data recommend the application of three polar liquids and a set of three equations, if the values of the liquids parameters, such as γ_{sv}^- or γ_{sv}^+ , are not too close.¹⁹ Della Volpe et al.²⁰ show that an improper utilization of the three liquids, without dispersive liquids, or with two prevalently basic or prevalently acidic liquids, strongly increases the ill-conditioning of the system. The different estimates of the acid–base components, obtainable for the same solid by different triplets of liquids, do not necessarily imply

TABLE IV
Surface Tension Parameters (mN/m) of the Liquids
Used for Contact Angle Measurements,
Red Blood Cells, and Platelets

Liquid	γ_{lv}	γ_{lv}^d	γ_{lv}^p	γ_{lv}^+	γ_{lv}^-
Water (W) ¹⁴	72.80	21.80	51.00	25.50	25.50
Formamide (F) ¹⁵	58.00	39.00	19.00	2.28	39.60
Methylene iodide (CH ₂ I ₂) ¹⁶	50.80	50.80	0	0.72	0
1-Brom-naphthalene (1-Bn) ¹⁷	44.40	44.40	0	0	0
Red blood cells ¹⁸	36.56	35.20	1.36	0.01	46.2
Platelets ¹⁸	118.24	99.14	19.10	12.26	7.44

TABLE V
Surface Tension Parameters (mN/m) and Contribution of the Polar Component to the Total Surface Tension (%) for Cellulose Acetate Films Prepared from Solutions in Acetone/Water (v/v %), According to the Acid/Base Method [eqs. (1)–(4)] for Untreated and Treated Samples

Samples	Untreated samples					Plasma-treated samples				
	γ_{sv}^d	γ_{sv}^p	γ_{sv}^+	γ_{sv}^-	γ_{sv}	γ_{sv}^d	γ_{sv}^p	γ_{sv}^+	γ_{sv}^-	γ_{sv}
CA _{1.73}	42.64	2.76	3.50	0.55	45.40	44.22	10.71	3.61	7.95	54.93
CA _{1.88}	40.32	3.83	3.29	1.39	44.15	43.96	11.25	3.61	8.76	55.21
CA _{1.90}	41.35	2.78	7.01	0.29	44.13	43.69	11.34	3.50	9.18	55.03
CA _{2.21}	42.64	2.64	3.36	0.52	45.08	43.69	10.56	3.80	7.34	54.25

that this method is inconsistent, but may simply reflect the large inaccuracies affecting the results, as due to ill-conditioning. Also, literature postulated²¹ that the contact angles should be measured with a liquid surface tension higher than the anticipated solid surface one, i.e., $\gamma_{lv} > \gamma_{sv}$. Equation (1), written for three liquids, leads to a three-equation system for determining the surface tension components. In our investigation, this system was simplified because according to Table IV, 1-bromo-naphthalene and methylene iodide are apolar solvents. Table V shows the results for surface tensions, where the disperse components, γ_{sv}^d , are higher than the polar one, γ_{sv}^p , characterized by high values of electron-acceptor parameters, γ_{sv}^+ , and lower values of the electron-donor parameters, γ_{sv}^- .

Besides this, the CA synthesis conditions, substitution degrees, history of the films formed from solutions, as well as their surface morphology can influence the results on surface tension parameters. Each AFM micrograph plotted in Figure 1 shows that the membrane surface is not smooth, pores and nodules of different size and intensity, and sometimes ordered domains being present. According to Table VI, the average values of pore characteristics and of the surface roughness parameters identified in

Figures 1 and 2 depend on the casting solutions in acetone/water non-solvent mixtures from which the films were prepared.

In addition, a previous article⁹ shows that decreasing of solvation power, observed from viscometric studies in dilute solution, and increasing of the gelation process detected by rheological data generates an increased pore number in the CA films.

Following the plasma treatment, the disperse component of surface tension, γ_{sv}^d , evidences a slight modification, while the total surface tensions, γ_{sv} , and the polar component of surface tension, γ_{sv}^p , increase, leading to higher values than those of the untreated ones. One should observe that, for the untreated samples, all solvents expressed in eq. (1) were used while, for the plasma treated samples, only F, CH₂I₂, and 1-Bn were used because increasing of hydrophilicity, as well as other effects generated by plasma treatment, induce high errors in the evaluation of water contact angle. Table V shows significant differences between the electron-donor parameters before and after plasma treatment. Thus, the electron-donor parameters are higher after plasma treatment, whereas the electron-acceptor parameter shows only insignificant changes. In addition, the apolar components slightly increase.

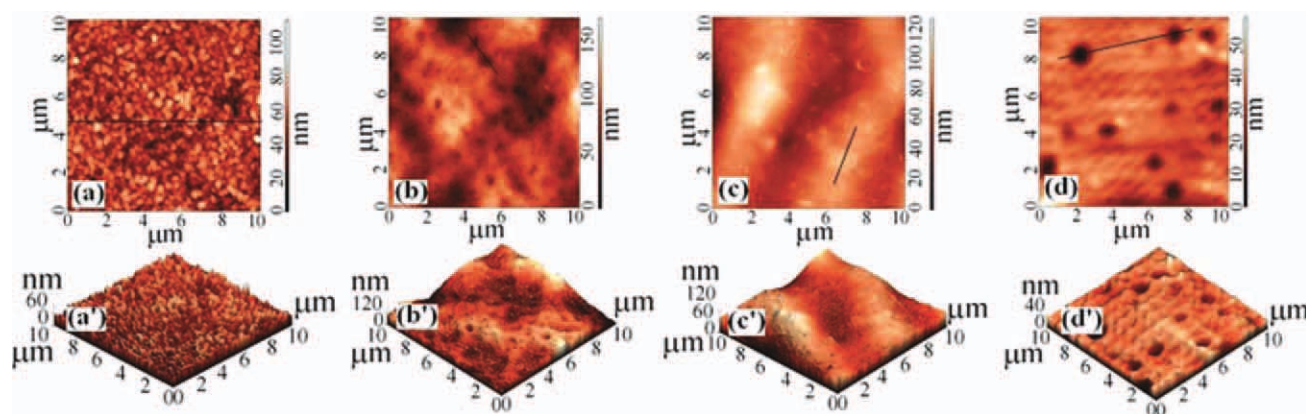


Figure 1 AFM images of membranes obtained from CA with different substitution degrees (DS) in acetone (1)/water (2) solvent mixtures: (a) 2D image, DS = 1.73, $\Phi_2 = 0.15$; (a') 3D image of (a); (b) 2D image, DS = 1.88, $\Phi_2 = 0.25$; (b') 3D image of (b); (c) 2D image, DS = 1.90, $\Phi_2 = 0.25$; (c') 3D image of (c); (d) 2D image, DS = 2.21, $\Phi_2 = 0.10$; (d') 3D image of (d). [Color figure can be viewed in the online issue, which is available at www.interscience.wiley.com.]

TABLE VI
Area (μm^2), Volume ($\mu\text{m}^2 \times \text{nm}$), Depth (nm), and Diameter (μm) of Pore Obtained from AFM Images, and Surface Roughness Parameters, Including Root-Mean-Square Roughness (rms, nm), Nodule Height from the Height Profile (nhp; nm) and Nodule Average Height from the Histogram (nhh; nm) of Membranes Prepared from Cellulose Acetates with Different Solvent Mixtures

Sample	Pore characteristics				Surface roughness		
	Area	Volume	Depth	Diameter	rms	nhp	nhh
CA _{1.73}	0.035	1.000	0.157	9.021	11.480	106	160
CA _{1.88}	0.206	8.464	0.275	7.287	5.833	78	70
CA _{1.90}	0.126	5.770	0.157	2.429	16.414	99	105
CA _{2.21}	0.640	12.203	0.784	11.797	4.525	40	110

Generally, a plasma treatment applied to cellulose derivative membranes induces modifications of surface properties because the highly energetic particles interact with the polymer surface. They may generate several kinds of reactions such as breakage of the covalent bonds along the chain, crosslinking, grafting, interactions of surface free radicals, alterations of the existing functional groups, and incorporation of chemical groups originating in plasma. Thus, one can assume, according to literature data that, during plasma treatment, some of the hydrogen bonds between the CA particles can be broken. At the same time, decreasing of the water contact angle values after plasma treatment indicates higher surface oxygenation, and thus, higher hydrophilicity.²²

Interfacial free energy and work of water spreading

The hydrophobicity of CA with different substitution degrees was also described by the interfacial free energy between the two sides of the CA film in water phase, ΔG_{sws} [eqs. (5) and (6)]:

$$\Delta G_{\text{sws}} = -2\gamma_{\text{sl}} \quad (5)$$

$$W_s = W_a - W_c = 2 \cdot [(\gamma_{\text{sv}}^d \cdot \gamma_{\text{lv}}^d)^{1/2} + (\gamma_{\text{sv}}^+ \cdot \gamma_{\text{lv}}^-)^{1/2} + (\gamma_{\text{sv}}^- \cdot \gamma_{\text{lv}}^+)^{1/2}] - 2 \cdot \gamma_{\text{lv}} \quad (6)$$

where γ_{sl} was calculated with eq. (4), W_a —work of water adhesion and W_c —work of water cohesion.

The parameter representing the solid–liquid interfacial tension, γ_{sl} takes positive values (Fig. 3). Moreover, the interfacial free energy, ΔG_{sws} evaluated from solid–liquid interfacial tension, γ_{sl} has negative values (Fig. 2). Therefore, an attraction occurs between the two surfaces of the same polymer, s , immersed in water, “ w ,” confirming the hydrophobic characteristics of the CA films. After plasma treatment, γ_{sl} presents smaller values and ΔG_{sws} higher values in comparison with the untreated samples, confirming increasing in hydrophilicity.

The hydrophilic/hydrophobic balance of these polymers was also described by the work of spreading of water, $W_{s,wr}$ [eq. (6)] over the surface, which represents the difference between the work of water adhesion, W_a and the work of water cohesion, W_c . According to the negative values of the interfacial free energy of CA, the work of spreading of water, $W_{s,wr}$ (Fig. 4), before and after plasma treatment, takes negative values, caused by the hydrophobic surfaces, where the work of water adhesion is lower, comparatively with the work of cohesion. At the same time, the plasma treatment determines an increase of $W_{s,wr}$ and thus, an increase of hydrophilicity.

Blood–cellulose acetate interactions

Blood compatibility is dictated by the manner in which the CAs surfaces interact with the blood constituents, such as red blood cells and platelets. To analyze the possibilities of using CA in biomedical applications, and for establishing their compatibility with blood, eq. (6) was used, where $W_{s,rbc}$ and $W_{s,p}$ describe the work of spreading of red blood cells and platelets¹⁸; when blood is exposed to a biomaterial surface, adhesion of cells, the extent of which decides the life of the implanted biomaterials, occurs; thus, cellular adhesion to biomaterial surfaces could activate coagulation and the immunological cascades. Therefore, cellular adhesion has a

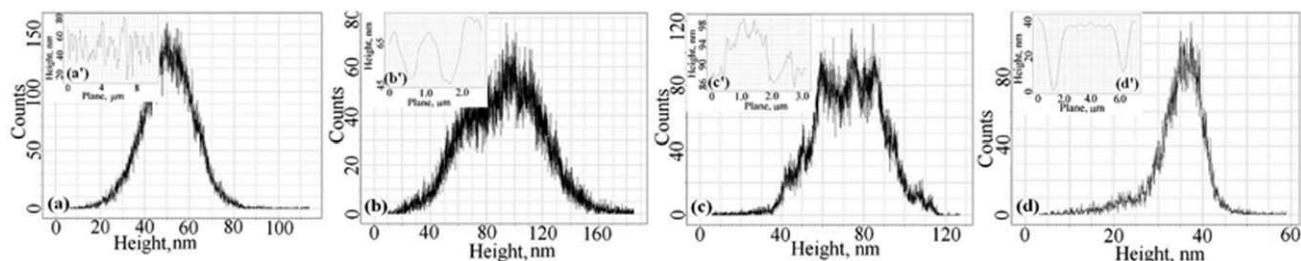


Figure 2 Histogram and surface profile (small plot) taken along a line from 2D AFM images of CA: (a) DS = 1.73, $\Phi_2 = 0.15$; (b) DS = 1.88, $\Phi_2 = 0.25$; (c) DS = 1.90, $\Phi_2 = 0.25$; (d) DS = 2.21, $\Phi_2 = 0.10$.

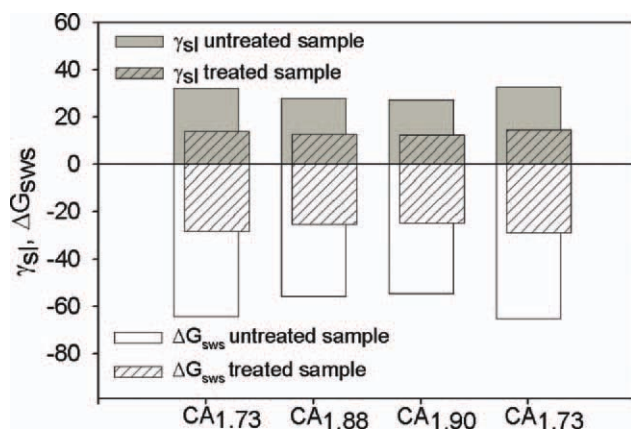


Figure 3 Solid–liquid interfacial tensions, γ_{sl} , and interfacial free energy, ΔG_{sws} , for CA with different substitution degrees.

direct bearing on the thrombogenicity and immunogenicity of a biomaterial, thus dictating its blood compatibility. In this article, the work of adhesion of the red blood cells was used as a parameter for characterizing biomaterials versus cell adhesion. The materials which exhibit a lower work of adhesion would lead to a lower extent of cell adhesion than those with a higher work of adhesion. Considering the surface energy parameters (γ_{lv} , γ_{lv}^d , γ_{lv}^+ , γ_{lv}^-) given in Table IV for red blood cells and platelets, the work of spreading of blood cells and platelets was estimated by eq. (7), with the surface free parameters for films prepared in nonsolvent/nonsolvent mixtures listed in Table V. Figure 4 shows positive values for the work of spreading of red blood cells, $W_{s, rbc}$, and negative values for the work of spreading of platelets, $W_{s, pr}$, suggesting a higher work of adhesion, comparatively with that of cohesion for the red blood cells, but a smaller work of adhesion, comparatively with the one of cohesion for platelets. On

the other hand, these results suggest that exposure of platelets to CA films determines an increase of platelets cohesion, which is higher for plasma treated films. In addition, Figure 5 shows the correlation between work of water, platelet, and red blood cell spreading versus root-mean-square roughness and pore volume of CA films with different substitution degrees. Note that, when the degree of substitution increases, roughness decreases, pore volume increases, while the works of water, platelet, and red blood cell spreading remain approximately constant.

Exception to this behavior occurs in the case of $CA_{1.90}$. For $CA_{1.88}$ and $CA_{1.90}$ films, evidencing close substitution degrees, the differences observed are consequences of the applied synthesis conditions (Table I). Thus, $CA_{1.90}$ is obtained through hydrolysis in media with lower water content, determining a lower amount of free OH groups, therefore a higher number of substituents at the primary carbon atom (C_6). The different distribution of substituents in both samples generated a higher hydrophobicity of the $CA_{1.90}$ membrane, comparatively with that of $CA_{1.88}$. In such a context, the work of spreading of red blood cell corresponding to the $CA_{1.90}$ film has higher values than for $CA_{1.88}$.

In summary, both red blood cells and platelets are extremely important in deciding the blood compatibility of a material. Moreover, it is known that adhesion of the red blood cells onto a surface, e.g. CA, requires knowledge of the interactions with the vascular components. Thus, endothelial glycocalyx, along with the mucopolysaccharides adsorbed on the endothelial surface of the vascular endothelium, reject the clotting factors and platelets—which have a significant role in thrombus formation.²³ In this context, adhesion of the red blood cells and cohesion of platelets to surface films should be discussed in correlation with future specific biomedical

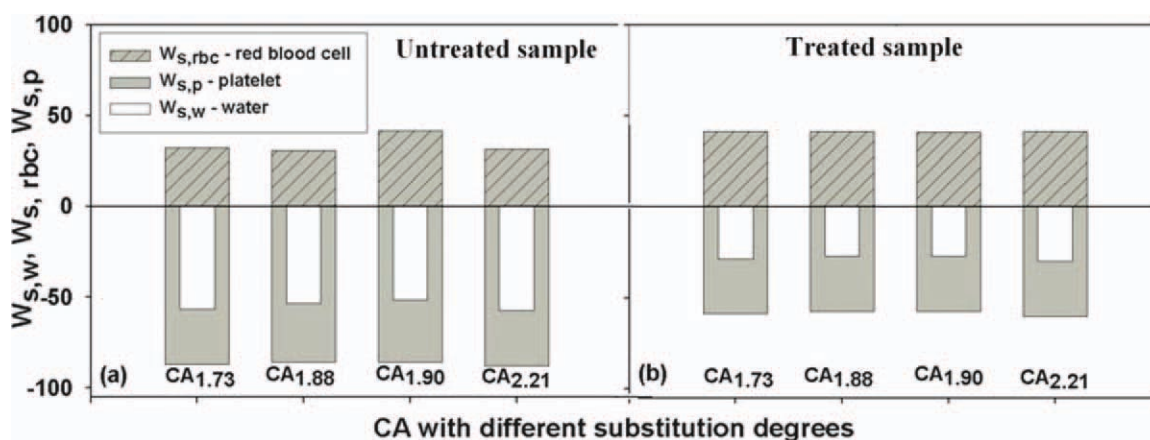


Figure 4 Work of water, red blood cells, and platelets spreading over the surface of CA films before and after plasma treatment.

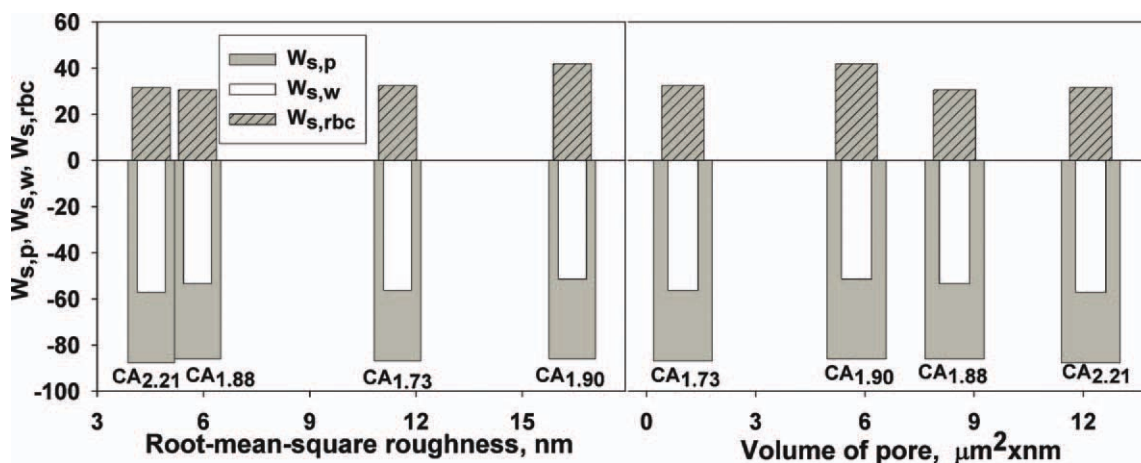


Figure 5 Work of water, platelet, and red blood cell spreading versus root-mean-square roughness and pore volume of CA films with different substitution degrees.

applications. These results seem to be applicable for evaluating bacterial adhesion to the surfaces, and could be subsequently employed for studying possible implanted-induced infections, or for obtaining semipermeable membranes.

CONCLUSIONS

CA was investigated to obtain information on their hydrophilic/hydrophobic properties and blood compatibility. The history of the formed films, prepared by a dry-cast process in acetone/water nonsolvent/nonsolvent mixtures, influenced the surface tension parameters, solid-liquid interfacial tension, interfacial free energy, as well as the work of water, and red blood cells and platelets spreading.

The results concerning the surface tension properties for both untreated and low-pressure plasma treated samples show that:

- the polar components obtained for each CA have a lower electron donor parameter, comparatively with the electron acceptor one, and also that the apolar components of surface free energy are higher than the polar components;
- generally, increase in the CA substitution degrees determines a decrease of hydrophilicity, even though the competition between the effect of the substitution degree, history of film preparations, and solution properties in mixed nonsolvents have generated some exceptions.
- low-pressure plasma treatment determines an increase of the polar component with the corresponding electron acceptor parameter, and thus an increase of hydrophilicity. Increasing of hydrophilicity by plasma treatment determines higher values of the work of water spreading.

On the other hand, for both untreated and plasma-treated samples, it was observed that:

- the work of red blood cells spreading, $W_{s,rbc}$, takes positive values, and the work of platelets spreading, $W_{s,p}$, takes negative values. Thus, the work of adhesion is higher than the work of cohesion of red blood cells, and the work of adhesion is lower, comparatively with the one of cohesion for platelets;
- plasma treatment determines an intensification of the work of red blood cells spreading and of the work of platelets spreading.

AFM images showed that surface morphology is characterized by roughness and nodules formations, depending on the composition of the nonsolvent/nonsolvent mixtures, including the characteristics of CA and the thermodynamic quality of the solvents. Moreover, the results suggest that surface hydrophobicity and surface roughness are controlling the compatibility with the red blood cells and platelets: a good hydrophobicity can be correlated with a good adhesion of the red blood cells and with a good cohesion of the platelets on the surface of the CA films.

These results are useful in investigations on specific biomedical applications, including evaluation of bacterial adhesion to the surfaces, and utilization of modified cellulose for semipermeable membranes in biomedical applications.

References

1. Entcheva, E.; Biana, H.; Yina, L.; Chunga, C.-Y.; Farrella, M.; Kostovc, Y. *Biomaterials* 2004, 25, 5753.
2. Eichhorn, S. J.; Baillie, C. A.; Zafeiropoulos, N.; Mwaikambo, L. Y.; Ansell, M. P.; Dufresne, A.; Entwistle, K. M.; Herrera-Franco, P. J.; Escamilla G. C.; Groom, L. *J Mater Sci* 2001, 36, 2017.

3. Hubbe, M. A.; Rojas, O. J.; Lucia, L. A.; Sain, M. *Biomaterials* 2008, 3, 929.
4. Pashkuleva, I.; Marques, A. P.; Vaz, F.; Reis, R. L. *J Mater Sci Mater Med* 2010, 21, 21.
5. Karahan, H. A.; Özdogan, E. *Fibers Polym* 2008, 9, 21.
6. Shao, D.; Jiang, Z.; Wang, X.; Li, J.; Meng, Y. *J Phys Chem B* 2009, 113, 860.
7. Pertile, R. A. N.; Andradea, F. K.; Alves, C., Jr.; Gama, M. *Carbohydr Polym* 2010, 82, 692.
8. Olaru, N.; Olaru, L. *J Appl Polym Sci* 2004, 94, 1965.
9. Necula, M. A.; Olaru, N.; Olaru, L.; Ioan, S. *J Macromol Sci Part B Phys* 2008, 47, 913.
10. Ioan, S.; Necula, A. M.; Olaru, N.; Olaru, L. *J Polym Charact* 2010, 15, 166.
11. Necula, M. A.; Olaru, N.; Olaru, L.; Homocianu, M.; Ioan, S. *J Appl Polym Sci* 2010, 115, 1751.
12. Tanghe, L. J.; Genung, L. B.; Mench, J. W. *Methods in Carbohydrate Chemistry*; R.L. Whistler: New York & London, 1963.
13. Rankl, M.; Laib, R.; Seeger, S. *Colloid Surf B* 2003, 30, 177.
14. Ström, G.; Fredriksson, M.; Stenius, P. J. *Colloid Interface Sci* 1987 119, 352.
15. van Oss, C. J.; Ju, L.; Chaudhury, M. K.; Good, R. J. *J Colloid Interface Sci* 1989, 128, 313.
16. Gonzalez-Martin, M. L.; Janczuk, B.; Labajos-Broncano, L.; Bruque, J. M. *Langmuir* 1997, 13, 5991.
17. Busscher, H. J.; van Pelt, A. W. J.; de Boer, P.; de Jong, H. P.; Arends, J. *Colloid Surf* 1984, 9, 319.
18. Vijayanand, K.; Deepak, K.; Pattanayak, D. K.; Rama Mohan, T. R.; Banerjee, R. *Trends Biomater Artif Organs* 2005, 18, 73.
19. Wu, W.; Giese, R. F., Jr.; van Oss, C. J. *Langmuir* 1995, 11, 379.
20. Della Volpe, C.; Maniglio, D.; Brugnara, M.; Siboni, S.; Morra, M. *J Colloid Interface Sci* 2004, 271, 434.
21. Kwok, D. Y.; Ng, H.; Neumann, A.W. *J Colloid Interface Sci* 2000, 225 323.
22. Filimon, A.; Avram, E.; Dunca, S.; Stoica, I.; Ioan, S. *J Appl Polym Sci* 2009, 112, 1808.
23. Reitsma, S.; Slaaf, D. W.; Vink, H. J.; van Zandvoort, M. A. M.; oude Egbrink, M. G. A. *Pflügers Archiv—Eur J Phys* 2007, 454, 45.